FORSCHUNGSZENTRUM KARLSRUHE
Technik und Umwelt

Wissenschaftliche Berichte
FZKA 5869

Gamma Irradiation-Corrosion Studies and Surface Analytical Investigations of the HLW Container Material Ti99.8-Pd

E. Smailos, D. Schild, K. Gompper
Institut für Nukleare Entsorgungstechnik

Work performed within the framework of the 1994-1998 programme of the European Atomic Energy Community: „Nuclear Fission Safety."
EU-Contract No. FI4W-CT95-0002

Forschungszentrum Karlsruhe GmbH, Karlsruhe
1997

SUMMARY

Previous corrosion studies identified the alloy Ti99.8-Pd as a promising material for the manufacture of long-lived high-level waste containers that could act as an engineered barrier in a rock-salt repository. In the present work, the combined influence of gamma radiation (10 Gy/h) and high temperature (150 °C) on the corrosion of Ti99.8-Pd in a disposal relevant $MgCl_2$-rich brine was investigated, and the corrosion films formed were characterized by XPS. For comparison, specimens without irradiation were also examined.

The corrosion results indicate that the passive corroded alloy Ti99.8-Pd is highly resistant to pitting and crevice corrosion in the brine, and its general corrosion is negligible low, both with and without irradiation. The thin corrosion films formed on the surface of unirradiated specimens and in the crevices of specimens exposed to radiation consist of TiO_2. However, outside the crevices of irradiated specimens, a oxide layer consisting of Mg (main component of the brine) and Si (impurity in the brine) oxide is built up over the TiO_2 layer. In general, the thickness of the TiO_2 layer increases non-linearly with corrosion time. Comparable TiO_2 layer thicknesses (30 - 65 nm, depending on the experimental conditions) are found for unirradiated and irradiated laboratory specimens. In the crevice areas of the irradiated specimens, the layer of the corrosion product is a factor of about 2 thicker than outside of the crevices. The TiO_2 layer formed on the in-situ corrosion specimens (33 nm / 5.3 years) is thinner than that of the laboratory specimens (58 nm / 191 days) indicating less agressive conditions than in the laboratory experiments.

In view of these results, the alloy Ti99.8-Pd continues to be considered as a strong candidate container material and will be further investigated.

KORROSIONSUNTERSUCHUNGEN UNTER GAMMA-BESTRAHLUNG UND OBERFLÄCHENANALYSEN AM HAW BEHÄLTERWERKSTOFF Ti99,8-Pd

ZUSAMMENFASSUNG

Bisherige Korrosionsuntersuchungen ergaben, daß die Legierung Ti99,8-Pd ein aussichtsreicher Werkstoff für langzeitbeständige Behälter zur Endlagerung von hochradioaktiven Abfällen ist. In der vorliegenden Arbeit wurde der kombinierte Einfluß von Gamma-Strahlung (10 Gy/h) und hoher Temperatur (150 °C) auf das Korrosionsverhalten des Werkstoffs in einer endlagerrelevanten $MgCl_2$-reichen Lösung untersucht und die gebildeten Korrosionsfilme mittels XPS charakterisiert. Zum Vergleich wurden auch Untersuchungen in Abwesenheit von Strahlung duchgeführt.

Die Ergebnisse der Korrosionsuntersuchungen zeigen, daß das passiv korrodierte Ti99,8-Pd sowohl mit als auch ohne Gamma-Bestrahlung eine hohe Resistenz gegenüber Loch- und Spaltkorrosion aufweist und daß seine Flächenkorrosion klein (< 1 µm/a) ist. Die auf der Oberfläche von unbestrahlten Proben und in den Spalten von bestrahlten Proben gebildeten dünnen Korrosionsschichten (Filme) bestehen aus TiO_2. Auf der frei korrodierten Oberfläche der bestrahlten Proben bildet sich über der TiO_2-Schicht eine Oxidschicht aus Mg (Hauptkomponente der Lösung) und Si (Verunreinigung in der Lösung). Die Dicke der TiO_2-Schicht nimmt mit der Korrosionszeit nicht linear zu, wobei nach einem Jahr für bestrahlte und unbestrahlte Laborproben vergleichbare Schichtdicken (30 - 65 nm je nach Prüfbedingungen) gemessen wurden. Im Spaltbereich der bestrahlten Proben ist die TiO_2-Schichtdicke etwa um den Faktor 2 größer als außerhalb des Spaltes. Die auf der In-Situ-Korrosionsprobe gebildete TiO_2-Schicht (33 nm / 5,3 Jahre) ist dünner als die auf der Laborproben (58 nm / 191 Tage), was auf eine geringere Korrosivität der In-Situ-Bedingungen gegenüber den Laborbedingungen hinweist.

Die Ergebnisse dieser Arbeit bestätigen frühere Untersuchungen, daß Ti99,8-Pd ein aussichtsreicher Behälterwerkstoff ist. Weitere Untersuchungen an diesem Werkstoff sind im Gange.

TABLE OF CONTENTS

1. INTRODUCTION AND OBJECTIVES

According to the German waste disposal concept, the heat-generating nuclear waste such as vitrified high-level waste and spent fuel will be disposed of in repositories located in deep rock-salt formations. The isolation of the radionuclides from the biosphere shall be ensured by a combination of geological, geoengineered and engineered barriers. One element of this multi-barrier concept, as a part of the engineered system, is the waste container (overpack). The main threat to container integrity is corrosion induced by contact with salt brines which may be present in the disposal area under certain conditions. Therefore, extended corrosion studies on various metallic materials have been undertaken at FZK/INE, Karlsruhe within the framework of the European Union research program aimed at identifying corrosion resistant materials for long-lived containers. The barrier function of such containers is important especially during the elevated-temperature phase in the disposal area, which lasts a few hundred years.

In previous corrosion studies on a wide range of materials in salt brines, the titanium alloy Ti99.8-Pd was identified as a strong candidate material for the manufacture of long-lived containers [1,2]. Its general corrosion in disposal-relevant salt brines was extremely low (< 1 µm/a) and the alloy exhibited a high resistance to local corrosion, such pitting. This excellent corrosion resistance in elevated-temperature environments is based on the formation of a very thin passive oxide surface film.

For a reliable evaluation of the corrosion behaviour of Ti99.8-Pd, further investigations are required to obtain information on the long-term stability of the passive layer under disposal-relevant conditions and the parameters affecting the corrosion process. An essential aspect of such investigations is the examination of the potential influence of gamma radiation exerted by the waste on the corrosion behaviour of the material. Among the questions of interest is information on the long-term stability of corrosion films to local corrosion, its composition and thickness, and the oxidation states of titanium.

Results of our irradiation corrosion-studies (10^3 Gy/h) on Ti99.8-Pd in brines at the lower temperature of 90 °C, and first findings of surface analyses of corrosion films formed under irradiation have been already reported in [3,4]. In the present study, the long-term behaviour of Ti99.8-Pd to pitting and crevice corrosion in brines was examined under more realistic disposal conditions at a high temperature of 150 °C and 10 Gy/h, and the corrosion films of several specimens were characterized in detail by XPS.

2. GAMMA IRRADIATION CORROSION STUDIES ON Ti99.8-Pd

Of the various types of radiation exerted by the waste, only gamma radiation is present at the surface of the container. The dose rate depends on the design of the container and the nature of the waste inside. For HLW containers acting as a radionuclide barrier in a rock-salt repository, a wall thickness of about 100 mm is needed for mechanical support against the rock pressure of 36 ± 5 MPa [5] at 1000 m disposal depth. In this case, the expected gamma dose rate on the surface of the container will be about 10 Gy/h. A such overpack which is under consideration consists of a mechanically stable steel container provided with a 3 - 4 mm corrosion protection layer of Ti99.8-Pd.

Corrosion studies under gamma irradiation are important for two reasons. Firstly, the interaction of gamma radiation with salt brines produces reduced/oxidized reactive particles and stable products such as e^-_{aq}, H_2, $Cl_2^{\bullet -}$, H_2O_2, ClO^-, etc. [6] which may change the rate and mechanism of corrosion. Secondly, the absorption of gamma radiation in the semi-conducting protective oxide layers of metals such as Ti99.8-Pd will induce photoradiation effects [7,8]. This ionization process may change the corrosion rate by increasing the carrier concentrations and facilitating cathodic/anoxic reactions at the oxide layer/electrolyte surface. Glass [8] concludes that the radiolytic products will exert the greatest effect on the corrosion process of metals.

To examine the combined influence of gamma radiation and high temperature on corrosion of Ti99.8-Pd in a disposal-relevant brine, both long-term immersion tests and detail investigations of the corrosion films formed were performed.

2.1 Material investigated and test conditions

The alloy Ti99.8-Pd was examined in the hot-rolled and annealed condition. The metal sheet used for the preparation of the corrosion specimens had the following composition in wt.%:
0.16 Pd; 0.03 Fe; 0.01 C; 0.15 O_2; 0.01 N_2; 0.001 H_2; bal. Ti.

For the corrosion studies, polished plane specimens of the dimensions 40 mm x 20 mm x 3 mm were used. General and pitting corrosion was investigated on single plane specimens, crevice corrosion on the contact surface of two plane specimens which were joined with a titanium bolt (metal/metal crevice corrosion). Prior to corrosion testing, all specimens were cleaned with alcohol in an ultrasonic bath.

The corrosion medium used was the $MgCl_2$-rich quinary „Q-brine“. The brine had at 55 °C the following composition in wt.%:
26.8 $MgCl_2$; 4.8 KCl; 1.4 NaCl; 1.4 $MgSO_4$; 65.7 H_2O.
The pH value of the brine at 25 °C was 4.6, and the dissolved O_2 1 mg/l.

The experiments lasted up to 1 year and were performed at a temperature of 150 °C which roughly corresponds to the maximum temperature on the surface of the containers according to the German disposal concept. The experiments under gamma radiation were performed at a dose rate of 10 Gy/h which is realistic for the thick-walled container discussed. For comparison, experiments without radiation have been also performed.

2.2 Experimental set-ups and post-test examination of the specimens

The corrosion experiments under gamma irradiation were performed in the spent fuel storage pool of KFA Jülich. The radiation source were spent fuel elements with a gamma energy spectrum similar to that of 10-years-old vitrified HLWC. The experimental set-up is shown schematically in Fig. 1. For the experiments, autoclaves made of the corrosion resistant alloy Ti99.8-Pd were used. The autoclaves provided with inserts made of quartz glass were placed in a circular configuration into heated cylindrical stainless steel containers (irradiation-containers). Each autoclave contained 120 ml of the brine and three specimens (40 mm x 20 mm x 3 mm) of 60 cm^2 total surface, which were totally immersed into the brine. This gave a brine volume to specimen surface ratio of 2 ml/cm^2. For irradiation, the stainless steel fuel containers were positioned at the bottom of the 6 m deep water-filled spent fuel element storage pool. The specimens and brines were heated to the test temperature of 150 °C using heaters.

For the experiments without irradiation (V/S = 2 ml/cm^2) at 150 °C, stainless steel pressure vessels provided with corrosion resistant insert vessels made of PTFE were used to avoid evaporation of the brine (boiling point: about 115 °C). These vessels were filled with brine, into which the specimens were immersed. After the pressure vessels had been closed, they were stored in heating chambers at 150 °C. The experiments were performed at equilibrium pressure of 0.4 MPa. To determine the corrosion kinetics, the specimens were examined at various immersion times.

After removal from the brine, the specimens were examined for general, pitting and crevice corrosion. The general corrosion was calculated from the gravimetrically determined weight losses and the material density. Evaluation of the specimens regarding pitting and crevice corrosion was carried out by surface profilometry and metallography. To obtain information on the potential effect of the various experimental test conditions which is necessary for predictions concerning the long-term corrosion behaviour of the material, a detailed characterization of the oxide surface layer of selected specimens was performed by means of XPS (see session 3).

2.3 Results

The results of the general corrosion obtained for Ti99.8-Pd after various exposure times to irradiated and unirradiated brines at 150 °C are compiled in Table 1. The data given for the weight losses and the integral corrosion rates are average values of three specimens. Over a test period of about 1 year the material corroded under the test conditions, as expected [1,2], at very low corrosion rates between 0.02 μm/a and 0.7 μm/a. The imposition of a 10 Gy/h radiation field on the 150 °C brine environment does not increase the corrosion rate of the material. A significant dependence of the corrosion rate on the corrosion time is not observed.

It is evident from the metallographic examinations and from the surface profiles of corroded specimens that the alloy Ti99.8-Pd is resistant to pitting corrosion both with and without irradiation. Under the test conditions, a completely uniform corrosion was observed. Characteristic optical micrographs of Ti99.8-Pd specimens after immersion in the brines at 150 °C are shown in Fig. 2.

The evaluation of the crevice specimens revealed general corrosion rates of about 0.05 μm/a which are close to the values of the gravimetric specimens. Moreover, the examination of the crevice area (contact metal to metal) did not show any signs of pitting corrosion. However, inside the crevice area a thin, multicolor corrosion product having yellow, violet and blue colors was observed. The examination of the various colored areas by XPS (see session 3) indicated in all cases TiO_2. This shows in accordance with the finding of Ahn and Soo [9] on Ticode12 in brine environments that the color differences of oxides inside the crevice area are due to optical interference colors caused by varying film thickness. Outside of the crevice, a very thin corrosion film having yellow color was formed.

3. SURFACE ANALYSES OF Ti99.8-Pd SPECIMENS

To obtain information on the potential effect of gamma irradiation and corrosion time on the behaviour of the Ti99.8-Pd in the test brine, the oxide surface film of selected specimens was investigated by means of XPS (X-ray Photoelectron Spectroscopy). This analytical method was selected since it has an information depth of a few nanometers, and it is applicable also to electric insulating surfaces. Together with ion sputtering, depth profiles of thin films can be acquired. In the present work, the composition and thickness of the corrosion surface layer were determined.

3.1 Experimental

The specimens investigated by XPS and the corrosion test conditions are given in Table 2. Both irradiated and unirradiated specimens were examined. Besides single plane specimens (gravimetric specimens), crevice specimens (contact metal to metal) were also examined. In the case of the crevice specimens, the inside (crevice area) as well as the outside (free corroded area) of the crevice were investigated. In addition to these investigations on laboratory specimens, a Ti99.8-Pd specimen stored under in-situ conditions in the Asse salt mine (5.3 years at 190 °C in rock salt plus migrated NaCl-rich salt brine) was analysed for comparison reasons.

Before analysis, the specimens were rinsed with destilled water, and in some cases additionally with ethanol. After drying at room temperature, the specimens were introduced into an ESCA (Electron Spectroscopy for Chemical Analysis) spectrometer from Physical Electronics type 5600ci for surface analysis. The spectrometer is equipped with a monochromator for Al Kα X-rays and a standard X-ray source with an aluminium and magnesium anode. A hemispherical electron analyser in the constant pass energy mode is used to record the spectra. The analysed area selected for the measurements has a diameter of 0.8 mm. A differentially pumped ion gun is used to remove material from the specimen surface by ion sputtering. The base pressure of the system is about 6×10^{-8} Pa and during acquisition of depth profiles about 4×10^{-6} Pa. In general, an angle of 45 degrees between the axis of the input

lens of the analyser and the surface normal of the specimen was used. Monochromated Al Kα X-rays were applied for survey and high resolution scans. Mg Kα radiation from the standard X-ray source was selected for survey scans and for XPS depth profiling. Due to the photo- and Auger electrons leaving the specimen surface, some specimens showed a surface charging, when the windowless X-ray monochromator was used. In this case, low energy electrons were applied to compensate the positive charging of the surface. The X-rays of the standard source were passing through an aluminium window from which secondary electrons were emitted. This supports the neutralization of the surface charge.

The elemental composition of the specimen surfaces was identified by recording XPS survey spectra at a constant pass energy of 187.85 eV of the electron analyser. Elemental concentrations were calculated from the peak areas of the photoelectron lines after background subtraction by use of atomic sensitivity factors described by Wagner et al. [10] and were adapted to the characteristics of the Omni Focus IV lens of the electron analyser. The concentrations were scaled to 100 %. The error of atomic concentrations is within 10 - 20 %.

XPS high resolution scans of core lines of the elements detected on the specimen surface give information about the chemistry of an element. The spectra of the lines were recorded before sputtering the surface. At a pass energy of 23.5 eV, the FWHM (Full Width at Half Maximum) of the $Ag3d_{5/2}$ line was 0.7 eV. The energy scale of the spectrometer was calibrated by the measurement of the $Au4f_{7/2}$, $Ag3d_{5/2}$ and $Cu2p_{3/2}$ lines of sputtered metal foils, respectively. A linear regression analysis between the measured data and the reference values of the $Au4f_{7/2}$, $Ag3d_{5/2}$ and $Cu2p_{3/2}$ lines [11] was used to correct the measured binding energies of the lines of the specimens. The lines are charge referenced to the C1s line of adventitious hydrocarbon at 284.8 eV [12]. The error in the determination of the line position is below 0.1 eV.

The axis of the ion gun was centred within the XPS analysis area by use of a video microscope, a slotted alignment sample, a Faraday cup and the scanning XPS

capability of the spectrometer. XPS depth profiles were acquired by alternate sputtering and recording of the core line spectra at a pass energy of 58.7 eV. The spectra acquired during the cycles of the depth profile were stored for analysis.

The ion gun was used with argon ions at an energy of 1 and 2 keV at an incident angle of 40 degrees to surface normal. The ion beam with a diameter of approximately 0.3 mm was rastered over a rectangular area of (3 x 3) mm^2. In addition, the specimen was rotated during sputtering with about 1 rotation per minute (Zalar Rotation™ [13,14,15]) to enhance the depth resolution by avoiding sputter-induced roughening of the specimen surface. The ion beam current with and without rastering was measured with a Faraday cup having an entrance hole with a diameter of 0.2 mm. For calibration of the sputter rate anodic oxidized reference films of Ta_2O_5 with 100 nm thickness on tantalum were used. The sputter rate was determined from the sputter time necessary to reduce the oxygen concentration to the half of its initial value. The depth resolution Δz of the apparatus was estimated from the difference between the sputter time at 84 % and 16 % of the O1s peak area [15].

3.2 Results

3.2.1 Investigations of unirradiated laboratory specimens

Surface composition

The surface composition of the polished specimens before and after exposure to brine at 150 °C was determined by recording XPS survey spectra covering the binding energy range from 0 to 1400 eV. The results obtained are summarized in Table 3. For comparison, also the results of surface analysis of in-situ specimens (see session 3.2.2) are given.

Figure 3 shows by way of example the XPS spectrum of a laboratory specimen corroded for 191 days in the brine at 150 °C. The surface constituents determined were:

- Ti, O are the main elements,
- Mg, Cl, S originate from the main components of the brine,
- Ca, Si are trace elements in the brine,
- C, N, Fe, and Zn originate from surface contamination

Figures 4 - 5 show high resolution spectra of the elemental core lines $Ti2p_{3/2}$ and O1s recorded before ion sputtering. Curve fitting was performed using Gauß-Lorentz curves after removal of a Shirley type background. The spectra were displayed with the original spectra, the background curve, the Gauß-Lorentz curves, the sum curve which fits the spectra, and the residual curve. The measured binding energies, the FWHM values and the peak areas for Ti and O are compiled in Table 4. For comparison, the literature values [12, 16] are also given. The corrosion film formed on the specimens assigned to TiO_2. The reasons are:

- The binding energies measured for Ti2p3/2 (458.2 ± 0.1 eV) and O1s (529.4 ± 0.1 eV) are very close to the reference values (458.5 - 459.0 eV for Ti2p3/2 and 529.7 - 530.2 eV for O1s) [12,16].

– The $Ti2p_{3/2}$ spectrum (Fig. 4) is fitted by one Gauß-Lorentz curve at 458.2 eV which indicates one chemical state.
– The O1s spectrum (Fig. 5) is fitted by two curves whereas the main line is located at 529.4 eV and the corresponding oxygen concentration is twice the titanium concentration. The second O1s line is assigned partly to Ca and Mg oxides and partly to C-OH and COOH groups of adventitious hydrocarbon.

Depth profiles and layer thickness

XPS depth profiles were recorded from selected specimens. In the following, the depth profile of the specimen described before (p. 9) will be discussed. This specimen was polished to a surface roughness of about 1 µm and subsequently was exposed for 191 days to Q-brine at 150 °C.

After one sputter cycle, the carbon concentration was reduced to less than 10 % of the value of the unsputtered surface and the elements N, Na, Cl, Mg, S, Zn and Fe disappeared. Therefore these elements are assigned to surface contamination. Si and C were still present at low concentrations.

The depth profile of the elements titanium, oxygen and carbon is shown in Fig. 6. After the first sputter cycle, the oxygen concentration is near to 66 at.% indicating the TiO_2 stochiometry. The depth profile shows a broad interface between the titanium oxide and the titanium bulk. This broadening can be attributed to several effects:

– The surface roughness (1 µm) is higher than the corrosion layer thickness (see below and Table. 5).
– The thickness of the corrosion layer is not homogeneous over the area analysed.
– At the oxide / metal interface oxygen diffusion into the bulk material takes place [17,18].
– Various crystalline phases of titanium oxide, as rutile and anatase can be present [19].

– Titanium reacts with oxygen from the residual gas of the vacuum chamber as the metal surface of titanium is high reactive. Therefore, the titanium and oxygen spectra were recorded at each cycle first.

Due to the above-mentioned reasons and the well known preferential sputtering of oxygen compared to titanium in the TiO_2 system [4,20,21], a determination of the layer thickness from the concentrations profiles (Fig. 6) is not reasonable. Therefore, the end of the oxide layer was characterized by the sputter cycle from which on no further shift of the peak maximum of the $Ti2p_{3/2}$ line to lower binding energy was observed, and metallic titanium dominated. The sputter time corresponding to this cycle is comparable with the sputter time at which the oxygen concentration drops to 50 % of the concentration after removal of the surface contamination.

For the estimation of the thickness of the corrosion layer, the actual sputter rate was determined by depth profiling of Ta_2O_5 reference films (Fig. 7). To convert the sputter rates of Ta_2O_5 to TiO_2, relative sputter rates were estimated from literature data [4,22,23] and using the density of the corresponding bulk materials. For argon ions at an energy of 2 keV, the following relative sputter rates result: Ta_2O_5: 1.0, TiO_2: 0.6, Ti: 0.7 and SiO_2: 0.8.

Under the above-mentioned considerations, a sputter time of 110 minutes and a sputter rate of 0.5 nm/min for TiO_2 were determined for the specimen. These values correspond to a layer thickness of 55 nm (see Table 5).

Taken into account the individual errors resulting from the depth resolution of the apparatus, the sputter process and the data analysis, the overall error of the depth analysis of the corrosion layers is estimated to be about 20 - 30 %.

3.2.2 Investigations of unirradiated in-situ specimens

In addition to laboratory specimens, an in-situ specimen was investigated. This specimen was stored for 5.3 years in a heated bore hole in the Asse salt mine at 190 °C. During the test duration the Ti99.8Pd-specimen was in contact with rock salt. Moreover about 1.1 litres of NaCl rich brine migrated into the borehole.

Surface composition

The material used for the specimen preparation had in the as-received condition a surface roughness of about 20 µm. After corrosion, the specimen surface was covered with a thin yellowish gold-colored film.

Figure 8 shows a XPS survey spectrum of the surface of the „in situ“ specimen. The surface analysis of corroded and uncorroded specimens revealed for both in principle the same elements. As in the case of the laboratory specimens, the main elements were titanium and oxygen. In addition C, Si, Fe, N, Mg, Al and traces of Cl, Zn, Cu and Pb were identified. In comparison to the parent material and to the laboratory specimens, the silicon concentration was enhanced by a factor up to about 14 (Table 3), which indicates that this element was present in the migrated rock salt brine.

High resolution spectra of the core lines of Ti2p and O1s are shown in Figs. 9 and 10. The measured binding energies and the literature data [12,16] are compared in Table 4. The analysis of the spectra was performed analogous to that for the laboratory specimens (see session 3.2.1). As in the case of the laboratory specimens, the $Ti2p_{3/2}$ spectrum is fitted by one Gauß-Lorentz curve and the O1s spectrum by two curves. The $Ti2p_{3/2}$ spectrum (binding energy 458.5 eV, FWHM 1.0 eV, pass energy of the analyser 5.85 eV) indicates one chemical state, namely TiO_2. In case of the O1s spectrum, the binding energy of 529.9 eV and the O/Ti ratio of 2 : 1 of the first curve indicate the presence of TiO_2. The second curve is assigned partly to oxygen of silicate and partly to C-OH and COOH groups of adventitious hydrocarbon.

Depth profiles and layer thicknesses

Depth profiles of the parent material and corroded specimens were accomplished with argon ions at 1 keV and 0.016 A/m^2 by Zalar Rotation™ (Figs. 11 - 12). In this case, sputter rates of 0.1 nm/min for TiO_2 and 0.12 nm/min for Ti were estimated. Si, C and the trace elements observed on the specimen surface were sputtered away after a few cycles. The estimation of the corrosion layer thicknesses (see session 3.2.1) leads to the following values: Parent material: 9 nm, corroded specimen: 33 nm.

3.2.3 Investigations of irradiated specimens

Surface analyses were performed on crevice specimens (contact metal to metal) exposed for various times to Q-brine at 150 °C and a gamma dose rate of 10 Gy/h. Both the crevice area and the free corroded specimen area were investigated. In the following, the results of surface composition and depth profiles obtained for a specimen corroded 8 months in the brine are discussed. Furthermore, results of the time-dependence of the corrosion layer thickness are reported.

Surface composition of the free corroded and crevice areas

The main elements observed on the free corroded specimen surface are carbon, oxygen, silicon (impurity in brine) and magnesium (main component of the brine) (Fig. 13). In addition, aluminium, iron, chlorine and nitrogen were observed at low concentrations. Titanium was not detected. The elements with their concentrations are compiled in Table 6. The measured binding energies compared to the reference values are given in Table 7. The high resolution O1s spectrum of the specimen surface is shown in Fig. 14.

The comparison of the binding energies for O1s, Si2p and Mg2p with literature data [12,16] and the determined element concentrations lead to the conclusion that SiO_2 and MgO or a magnesium silicate compound may be present. On the basis of the measured binding energies the presence of $Mg(OH)_2$ can be excluded. As the Si content is enhanced compared to unirradiated specimens, it cannot be excluded that a part of Si results from the corrosion of the autoclaves quartz glass inserts that were used instead of the radiation unstable PTFE liners.

XPS analysis of the crevice area shows that besides carbon, oxygen and silicon, titanium is present as a main component (Fig. 15). For titanium and silicon the same concentrations of about 7 at.% were found. In contrast to the free corroded area, magnesium was present only as a trace element. Further elements found in low concentrations are given in Table 6.

Figures 16 - 17 show XPS spectra of $Ti2p_{3/2}$ and O1s taken from the crevice area. The binding energies (Tab. 7) and the O/Ti ratio indicate as in the unirradiated specimen the presence of TiO_2. The examination of the various colored areas inside the crevice does not indicate changes in the titanium oxide composition. The binding energy of the Si2p line (102.1 eV) is not in line with the reference value of SiO_2 (103.3 - 103.7 eV) but such values are typical for silicate compounds. The values of the binding energies for $Ca2p_{3/2}$ and the $Zn2p_{3/2}$ are assigned to CaO and ZnO, respectively.

Depth profiles and layer thicknesses of free corroded and crevice areas

Figure 18 shows the depth profile of the free corroded area of the specimen discussed before. The sputtered surface shows silicon and magnesium as observed by the survey spectra recorded before sputtering. In addition, titanium was observed from the first sputter cycle on with continuous rising peak intensity. The corrosion layer consists of silicon, magnesium and titanium oxides. No sharp transition between a silicon-magnesium oxide layer and a titanium oxide layer was observed in the depth profile. A similar result was obtained also by G. Pfennig et al. [4] on a

Ti99,8-Pd specimen corroded in Q-brine at the lower temperature of 90 °C and high gamma radiation (10^3 Gy/h). In this case, the titanium oxide layer can be estimated by the difference between the sputter time at which the silicon concentration is diminished to the half of the initial concentration (150 min), and the sputter time from which on a constant binding energy of the $Ti2p_{3/2}$ line is observed (280 min). From the sputter time difference and the sputter rate of TiO_2 (0.5 nm/min) a layer thickness of 65 nm was estimated.

In the case of the crevice area, besides TiO_2 a thin film of silicate was detected at the specimen surface (Fig. 19). After a few sputter cycles, the corrosion layer consisted only of titanium dioxide. The thickness of the TiO_2 layer was estimated to be 83 nm. The estimated TiO_2 -layer thicknesses for irradiated and unirradiated specimens are compiled in Table. 5.

The comparison of the values shows that the corrosion of the unirradiated specimens are very close to those of irradiated specimens. This result is in good agreement with the finding of Y.J. Kim and R.A. Oriani [19] observed on the titanium alloy Ticode 12 after corrosion in a disposal relevant brine. In case of the irradiated crevice specimens, the corrosion in the crevice area appears to be some higher than in the free corroded area.

4. CONCLUSIONS

The results of this study confirm previous findings that the alloy Ti99.8-Pd is a strong candidate material for the manufacture of long-lived high-level waste containers. In the test brine at 150 °C with and without gamma radiation the passive corroded material is highly resistant to pitting and crevice corrosion, and its general corrosion is very low.

The corrosion film formed on the surface of specimens tested without irradiation consists of TiO_2. Also the corrosion product formed in the crevices of specimens

exposed to radiation is TiO_2. However, outside the crevices (free corroded areas) of irradiated specimens, a layer consisting of SiO_2 and MgO or a magnesium-silicate compound is built up over the TiO_2 layer. Mg is a main component of the brine and Si is present as impurity in the brine. Nevertheless, as the Si content is enhanced compared to unirradiated specimens, it cannot be excluded that a part of Si results from the corrosion of the autoclaves glass inserts that were used instead of the radiation unstable PTFE liners.

In general, a non-linear increase of the TiO_2 layer thickness with corrosion time was observed. The TiO_2 layer thickness of unirradiated and irradiated laboratory specimens are comparable (about 30 - 65 nm, depending on the experimental conditions). In the crevice areas of the irradiated specimens, the thickness of the corrosion product is a factor of about 2 thicker than outside of the crevices. The TiO_2 layer formed on the in-situ corrosion specimens (33 nm / 5.3 years) is thinner than that of the laboratory specimens (58 nm / 191 days) indicating less agressive conditions than in the laboratory experiments. The very thin TiO_2 corrosion layers determined by XPS show in agreement with the gravimetric analyses that under test conditions corrosion of Ti99.8-Pd is very small.

Further investigations of Ti99.8-Pd are in progress. These involve above all the examination of the synergistic effect of gamma radiation and salt impurities (e.g. $B(OH)_4^-$, S^{2-}) on corrosion, the determination of the influence of welding on corrosion, and the performance of stress corrosion cracking studies.

ACKNOWLEDGMENTS

The authors wish to thank Mrs. R. Weiler and Mr. B. Fiehn for the technical assistance, and the Commission of the European Union, Brussels, Belgium, for financial supporting this work.

5. REFERENCES

[1] G.P. Marsh, G. Pinard-Legry, E. Smailos, F. Casteels, K. Vu Quang, J. Cripps, B. Haijtink, „HLW Container Corrosion and Design," Proc. of the Second European Community Conference on Radioactive Waste Management and Disposal, Luxembourg, April 22-26, 1985, p. 314, RA. Simon, [Ed.], Cambridge University Press (1986).

[2] E. Smailos, W. Schwarzkopf, and R. Storch, „Corrosion Studies of Packaging Materials for High-Level Waste Disposal in a Rock-Salt Repository," P.J. Tunturi [Ed.], Proc. Of the 12th Scandinavian Corrosion Congress and EUROCORR'92, SF, May 31-June 4, 1992, Vol II, p. 327. The Corrosion Society of Finland (1992).

[3] E. Smailos, R. Köster, „Corrosion Studies on Selected Packaging Materials for Disposal of High-Level Wastes," Proc. Of a Technical Committee Meeting on Materials Reliability in the Back End of the Nuclear Fuel Cycle organized by the IAEA, Vienna 2-5 September 1986, IAEA-TECDOC-421 (1987) 7-24.

[4] G. Pfennig, H. Moers, H. Klewe-Nebenius, R. Kaufmann and H.J. Ache, „Surface Analytical Investigation of the Corrosion Behaviour of Ti(Pd) Samples," Microchimica Acta [Wien], Suppl. 11, (1985) 113-124.

[5] A. Pudewills, E. Korthaus, and R. Köster, „Model Calculations of the Thermomechanical Effects in the Near Field of a High Level Radioactive Waste Repository," Proc. Symp. Waste Management '88, Tucson, Arizona, February 28-March 3, 1988, Vol. 2, p. 691, Arizona Board of Regents (1988).

[6] G.H. Jenks, „Radiolysis and Hydrolysis in Salt-Mine Brines," ORNL-TM-3717, Oak Ridge National Laboratory (1977).

[7] A.V. Bjalobzeskij, „Korrosion durch radioaktive Strahlung," in K. Schwabe (ed.), Akademie Verlag, Berlin, p. 82 (1971).

[8] R.S. Glass, „Effect of Radiation on the Chemical Environment Surrounding Waste Canisters in Proposed Repository Sites and Possible Effects on the Corrosion Process," SAND 81-1677 (1981).

[9] T.M. Ahn and P. Soo, „Container Assessment: Corrosion Study of HLW Container Materials," NUREG/CR-2317, BNL-NUREG-51449, Vol. 1, No. 4, Brookhaven National Laboratory (April 1983).

[10] C.D. Wagner, L.E. Davis, M.V. Zeller, J.A. Taylor, R.H. Raymond, L.H. Gale, „Empirical Atomic Sensitivity Factors for Quantitative Analysis by Electron Spectroscopy for Chemical Analysis," Surface Interface Anal. 3(5) (1981) 211-225.

[11] M.P. Seah, „Post-1989 Calibration Energies for X-ray Photoelectron Spectrometers and the 1990 Josephson Constant," Surface Interface Anal. 14 (1989) 488.

[12] J.F. Moulder, W.F. Stickle, P.E. Sobol, K.D. Bomben, „Handbook of X-ray Photoelectron Spectroscopy," (ed. J. Chastain) Perkin-Elmer Corporation, Physical Electronics Devision, Eden Prairie, Minnesota, USA (1992) and references herein.

[13] A. Zalar, „Improved Depth Resolution by Sample Rotation during Auger Electron Spectroscopy Depth Profiling," Thin Solid Films 124 (1985) 223-230.

[14] S. Hofmann, A. Zalar, E.-H. Cirlin, J.J. Vajo, H.J. Mathieu and P. Panjan, „Interlaboratory Comparison of the Depth Resolution in Sputter Depth Profiling of Ni/Cr Multilayers With and Without Sample Rotation using AES, XPS and SIMS," Surface Interface Anal. 20 (1993) 621-626.

[15] S. Hofmann, „Approaching the Limits of High Resolution Depth Profiling," Appl. Surf. Sci. 70/71 (1993) 9-19.

[16] C.D. Wagner, D.M. Bickham, „NIST X-ray Photoelectron Spectroscopy Database," NIST (National Institute for Standards and Technology) Standard Reference Database 20, Ver. 1.0 (1989).

[17] T.N. Wittberg, J.D. Wolf, R.G. Keil, P.S. Wang, „Low-Temperature Oxygen Diffusion in Alpha Titanium Characterized by Auger Sputter Profiling," J. Vac. Sci. Technol. A 1(2) (1983) 475-478.

[18] J.W. Rogers, Jr, K.L. Erickson, D.N. Belton, R.W. Springer, T.N. Taylor and J.G. Beery, „ Low Temperature Diffusion of Oxygen in Titanium and Titanium Oxide Films," Appl. Surface Sci. 35 (1988-89) 137-152.

[19] Y.J. Kim, R.A. Oriani, „Corrosion Properties of the Oxide Film Formed on Grade 12 Titanium in Brine Under Gamma Irradiation," Corrosion 43 (2) (1987) 85-91.

[20] U. Bardi, K. Tamura, M. Owari and Y. Nihei, „Angular Resolved X-ray Photoemission Study of Defects Induced by Ion Bombardment on the TiO_2 Surface," Appl. Surf. Sci. 32 (1988) 352-362.

[21] T. Albers, M. Neumann, D. Lipinsky and A. Benninghoven, „XPS and SIMS/SNMS Measurements on Thin Metal Oxide Layers," Appl. Surface Sci. 70/71 (1993) 49-52.

[22] H.H. Andersen and H.L. Bay, „Sputtering Yield Measurements" in „Sputtering by Particle Bombardment I," Topics in Applied Physics (ed. R. Behrisch) Vol. 47 (1981) 145-218, Springer-Verlag Berlin, Heidelberg, New York.

[23] M.P. Seah, M.W. Holbourn, C. Ortega and J.A. Davies, „An Intercomparison of Tantalum Pentoxide Reference Studies," Nucl. Instr. Meth. Phys. Res. B30 (1988) 128-139.

Table 1. Corrosion of Ti99.8-Pd in $MgCl_2$-rich brine (Q-brine) at 150 °C with and without gamma radiation field

Dose rate [Gy/h]	Exposure time [days]	Weight loss *) [mg]	Corrosion rate *) [µm/a]
0	63	0.10 ± 0.04	0.09 ± 0.04
	125	0.06 ± 0.06	0.02 ± 0.02
	191	3.50 ± 0.02	0.73 ± 0.01
	268	0.10 ± 0.04	0.02 ± 0.01
10	63	0.10 ± 0.10	0.06 ± 0.06
	174	0.62 ± 0.09	0.14 ± 0.02
	244	3.79 ± 0.06	0.62 ± 0.01
	356	1.49 ± 0.14	0.21 ± 0.02

*) average value of three specimens

Table 2. Ti99.8-Pd specimens analysed by XPS

Type of specimen	Corrosion conditions
Laboratory plane specimens	– Parent material – Q-brine / 150 °C / 63, 191 days
In-situ specimens	– Parent material – Asse salt brine / 190 °C / 5.3 years
Crevice specimens (metal/metal contact) Free corroded and crevice area	– Q-brine / 150 °C / 10Gy/h / 63, 69, 174, 244, 293, 356 days

Table 3. Elements and their concentrations at the surface of Ti99.8-Pd specimens before sputtering

Elements	Laboratory plane specimens		In-situ specimens	
	Parent material [at.%]	(Q-brine 150°C/191d) [at.%]	Parent material [at.%]	(NaCl brine 190°C/5.3a) [at.%]
O	49.2	36.2	43.0	51.5
C	27.8	46.6	34.4	23.3
Ti	15.2	11.0	15.4	8.6
Si	0.7	0.8	0.5	7.2
Fe		0.5		2.9
N	1.1	1.1	2.7	2.5
Mg	0.7	0.7	0.6	1.4
Al				1.1
Cl	0.3	0.6	0.3	0.8
Zn	2.6	0.6	0.3	0.4
Cu			1.2	0.2
Pb			1.4	0.1
Pd			0.2	
Ag			0.1	
Ca	2.0	1.6		
S	0.5	0.5		

Table 4. Binding energies (BE), FWHM values and peak area amounts for Ti, O and Si photoelectrons (error of binding energies: ± 0.1 eV)

Compound	Reference [12,16]	Measured in this work					
		Laboratory plane specimen (Q-brine / 150 °C / 191 days)			In-situ specimen (NaCl brine / 190 °C / 5.3 years)		
	BE [eV]	BE [eV]	FWHM [eV]	area [%]	BE [eV]	FWHM [eV]	area [%]
O1s							
TiO_2	529.7 - 530.2	529.4	1.2	66	529.9	1.1	36
CaO MgO Hydroxide Silicate	529.4 - 531.3 530.0 - 532.1 530.9 - 532.0 531.2 - 532.8	531.3	2.1	34	531.8	2.2	64
$Ti2p_{3/2}$							
TiO_2	458.5 - 459.0	458.2	1.1	100	458.5	1.0	100
Si2p							
Silicate	102.0 - 103.1	low concentration			102.7	1.8	100
$Ca2p_{3/2}$							
CaO	346.1 - 347.3	346.9	1.5	100	traces		

Table 5. Layer thickness of TiO_2 versus corrosion time for Ti99.8-Pd specimens*) exposed to Q-brine at 150 °C (estimated error ± 20 %)

Corrosion time	Layer thicknesses		
	Unirradiated specimens	Irradiated specimens (10 Gy/h)	
		Free corroded area	Crevice area
[days]	[nm]	[nm]	[nm]
0	6	6	6
63	28	41	
69		36	89
174		40	55
191	55		
244		65	83
293		44	75
356			86

*) polished specimes

Table 6. Comparison of the compositions of the free corroded and crevice surface of an irradiated Ti99.8-Pd specimen (Q-brine,150 °C, 10 Gy/h, 244 days)

Elements	Free corroded area [at.%]	Crevice area [at.%]
O	49.8	34.0
C	23.8	48.8
Ti		7.0
Si	14.1	7.1
Mg	10.2	
Al	1.1	
Ca		1.0
Cl	0.4	
N	0.6	1.3
Zn		0.7

Table 7. Binding energies (BE), FWHM values and area amounts of various photoelectron lines for an irradiated Ti99.8-Pd crevice specimen (Q-brine, 150 °C, 10 Gy/h, 244 days) (error of binding energies: ± 0.1 eV)

Compound	Reference [12,16] BE [eV]	Measured in this work					
		Free corroded area			Crevice area		
		BE [eV]	FWHM [eV]	area [%]	BE [eV]	FWHM [eV]	area [%]
O1s							
TiO_2	529.7 - 530.2	not detected			529.7	1.3	51
Hydroxide Silicate Silica	530.9 - 532.0 531.2 - 532.8 532.4 - 533.2	532.9	2.6	100	532.1	1.9	49
$Ti2p_{3/2}$							
TiO_2	458.5 - 459.0	not detected			458.4	1.1	100
Si2p							
Silicate Silica	102.0 -103.1 103.3 - 103.7	103.6	2.4	100	102.1	1.5	100
$Ca2p_{3/2}$							
CaO	346.1 - 347.3	not detected			347.3	1.6	100
Mg2p							
MgO	50.8	50.8	2.4	100	traces		
$Zn2p_{3/2}$							
ZnO	1021.4 - 1022.0	not detected			1021.8	1.6	100

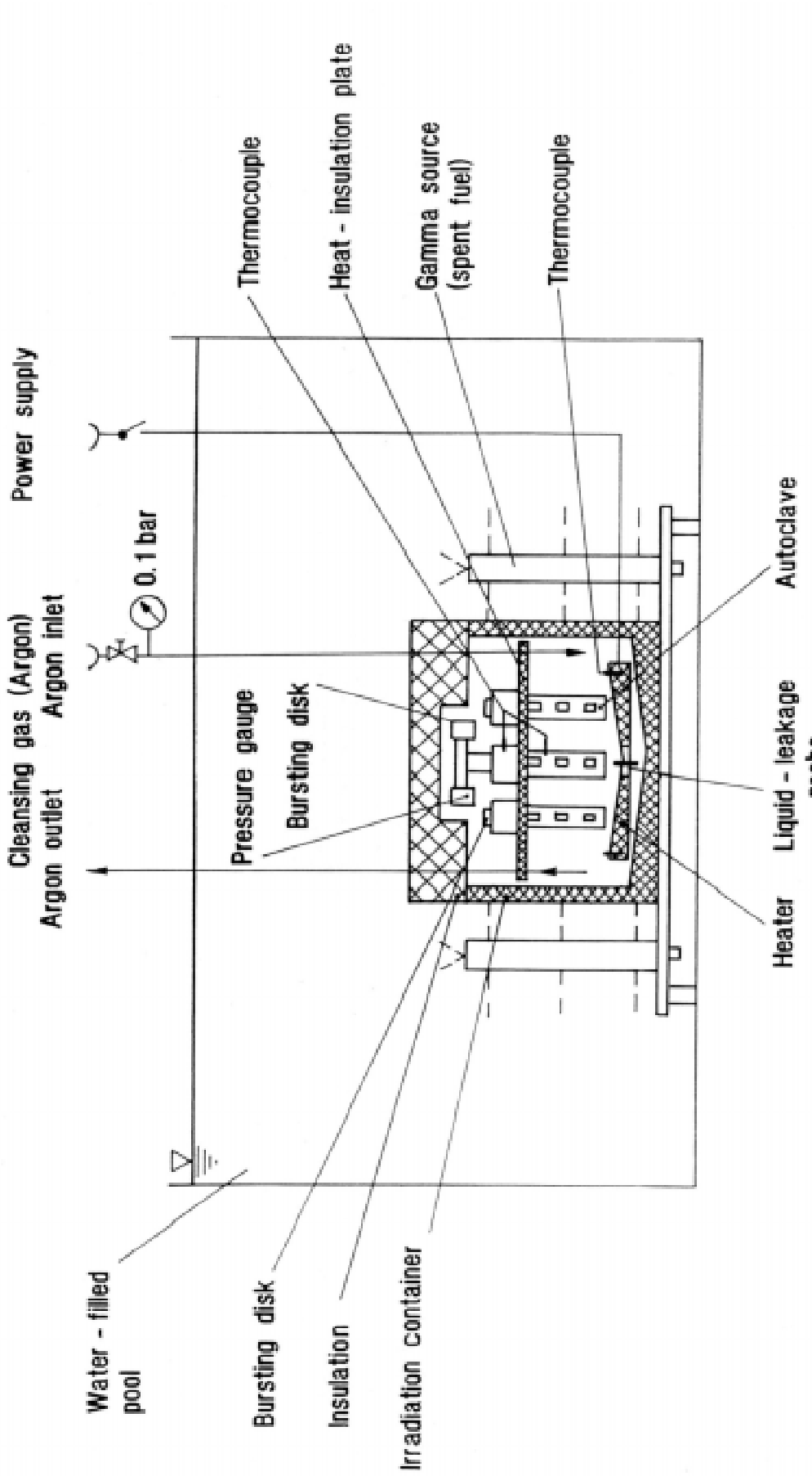

Fig. 1. Schematic of irradiation-corrosion test facility

Fig. 2. Optical micrographs of Ti99.8-Pd after corrosion in $MgCl_2$-rich Q-brine at 150 °C with and without gamma irradiation

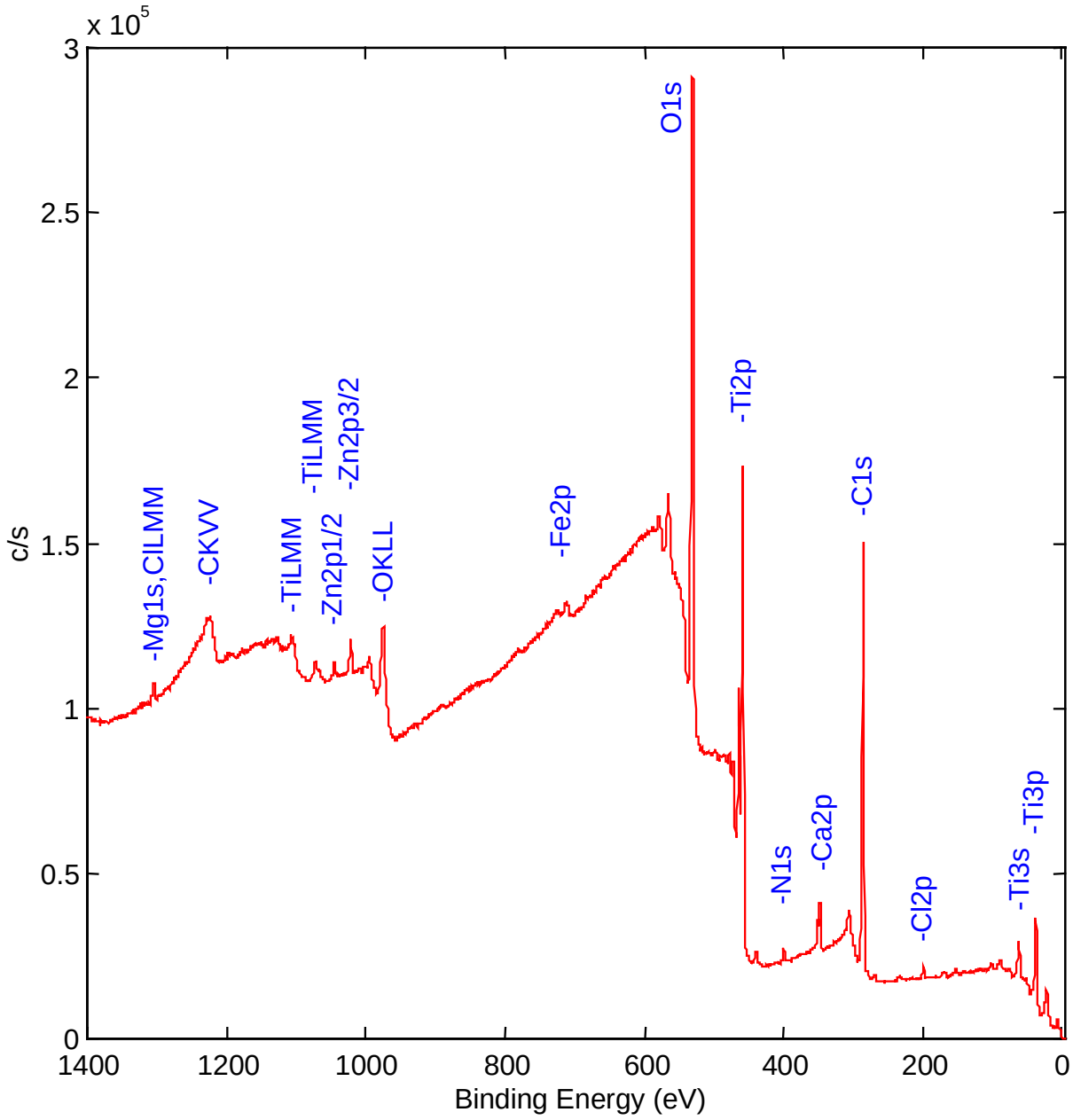

Fig. 3. XPS survey spectrum of a Ti99.8-Pd specimen exposed for 191 days to Q-brine at 150 °C (spectrum excited by Al Kα X-rays)

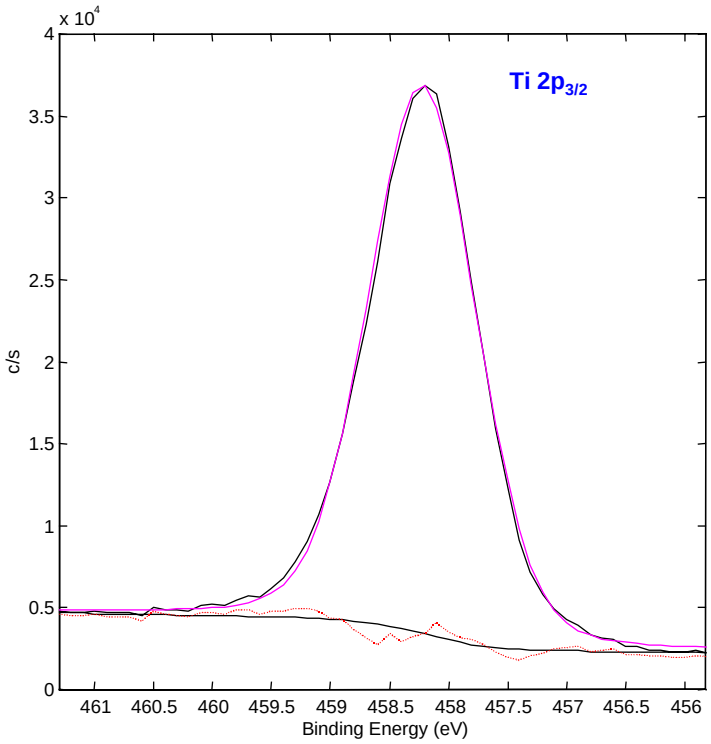

Fig. 4

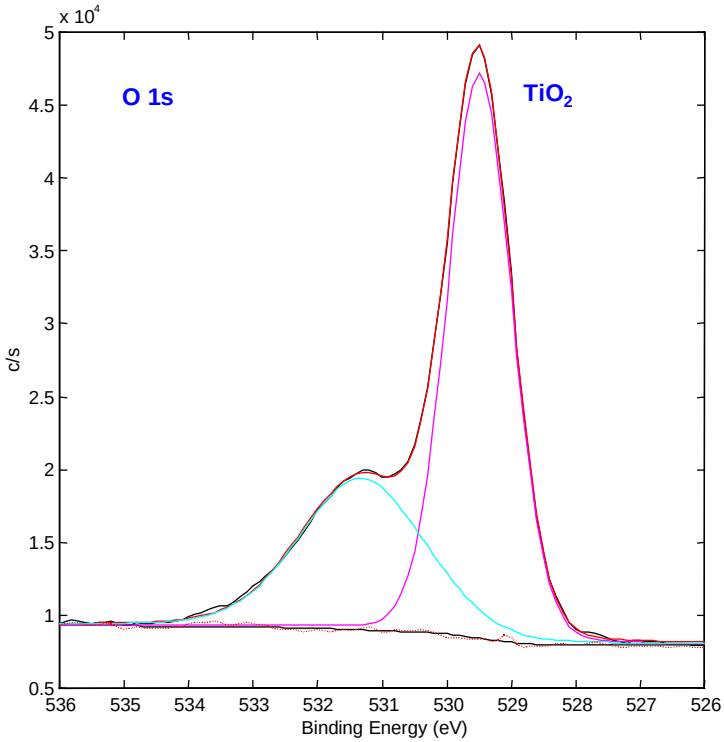

Fig. 5

Figs. 4 - 5. $Ti2p_{3/2}$ (Fig. 4) and O1s (Fig. 5) spectra of a Ti99.8-Pd specimen (191 days in Q-brine at 150 °C) displayed with the result of the curve fitting

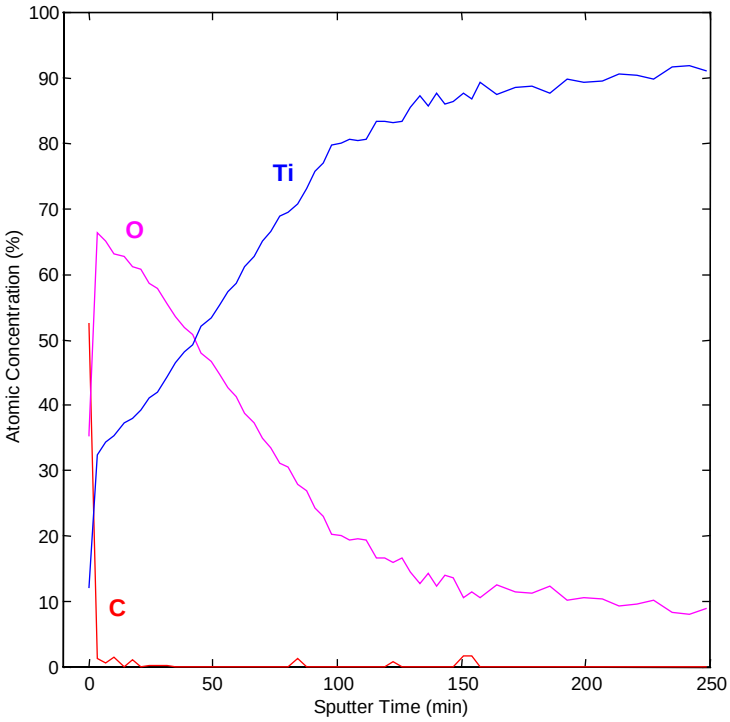

Fig. 6. Depth profile of a Ti99.8-Pd specimen (191 days in Q-brine at 150 °C). Atomic concentrations of Ti, O and C versus sputter time. The experimental sputter rates amount to 0.5 nm/min for TiO_2 and 0.58 nm/min for Ti

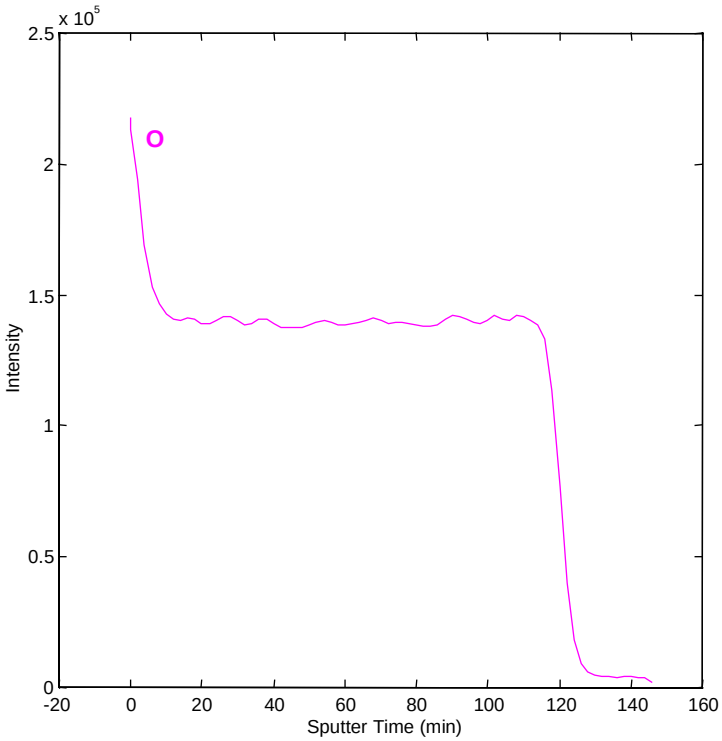

Fig. 7. Oxygen depth profile of the Ta_2O_5 reference film (thickness 100 nm, sputter rate of Ta_2O_5 0.83 nm/min, depth resolution $\Delta z \approx 4.1$ nm)

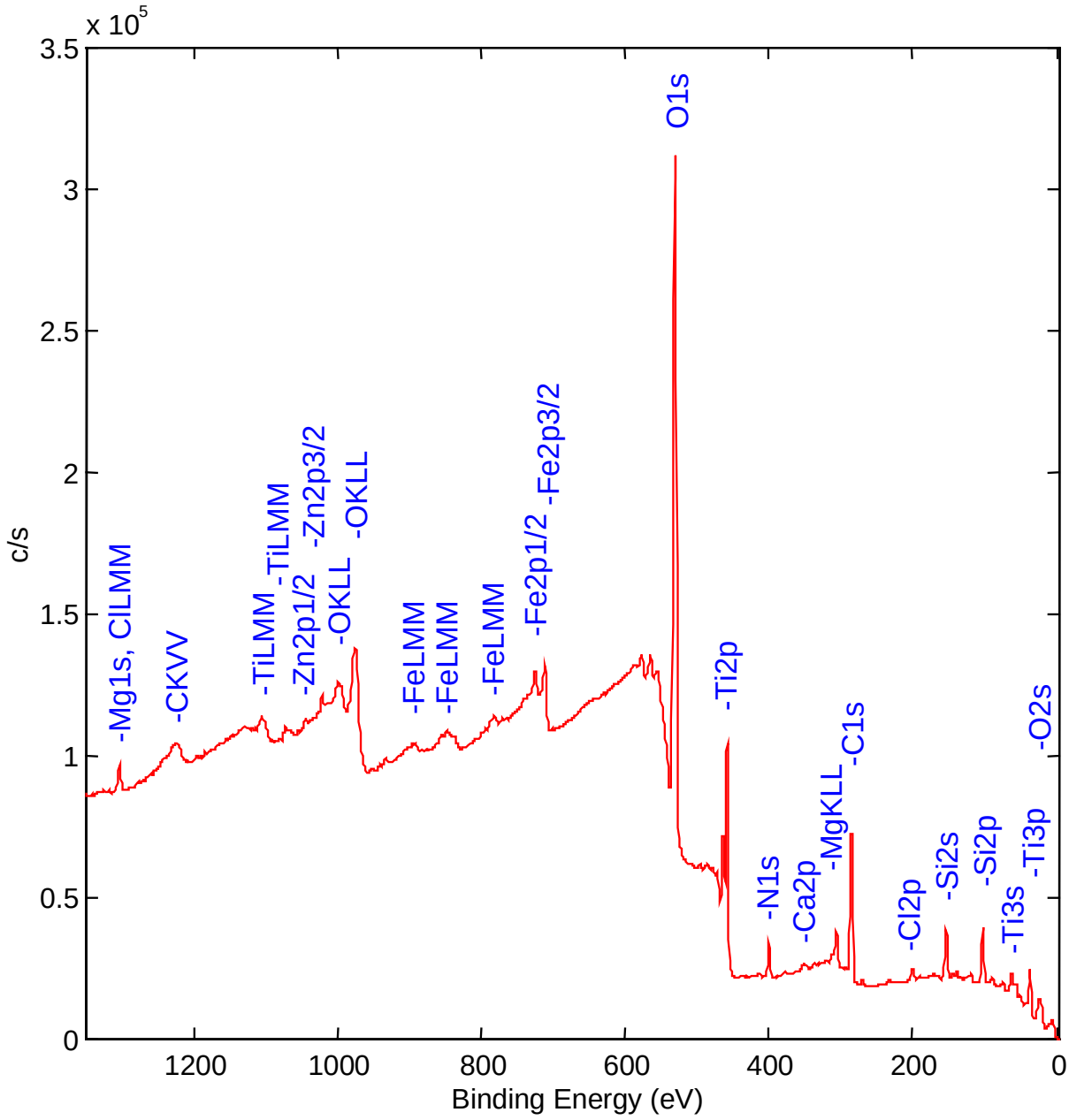

Fig. 8. XPS survey spectrum of the Ti99.8-Pd in-situ specimen tested in the Asse salt mine (5.3 years at 190 °C in rock salt brine)

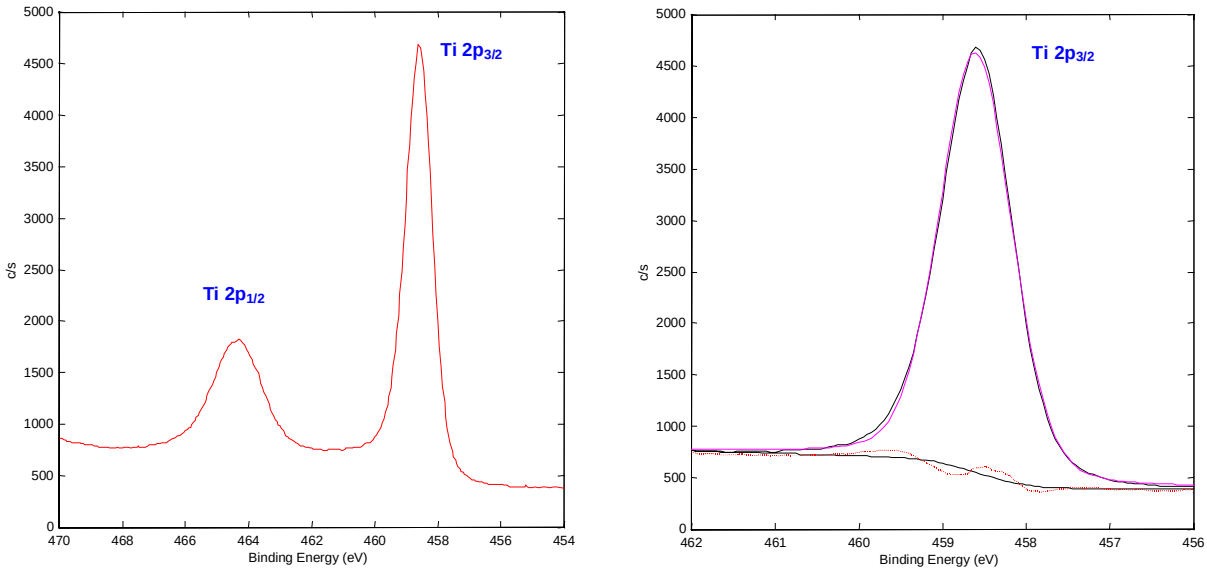

Fig. 9. Ti2p spectrum and curve fit of the $Ti2p_{3/2}$ peak indicating TiO_2 at the surface of the in-situ specimen

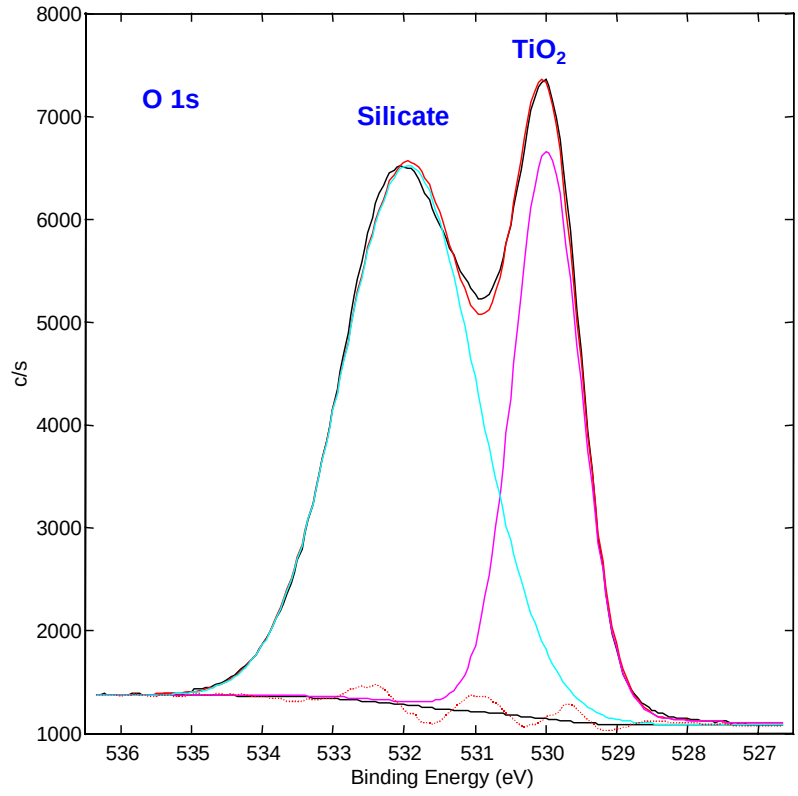

Fig. 10. The O1s spectrum of the in-situ specimen indicating silicate and TiO_2

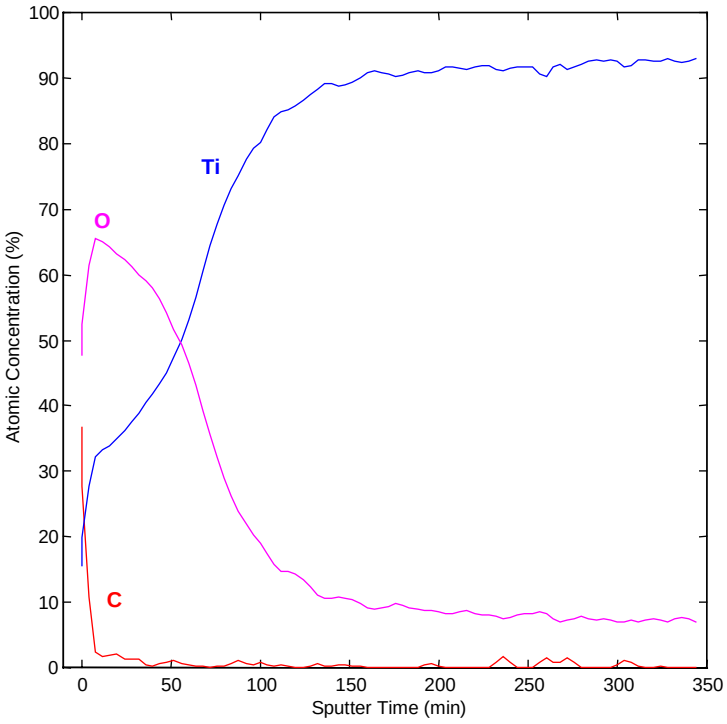

Fig. 11. Depth profile of the parent material used for the in-situ corrosion studies (roughness 20 µm). The experimental sputter rates amount to 0.12 nm/min for TiO_2 and 0.14 nm/min for Ti

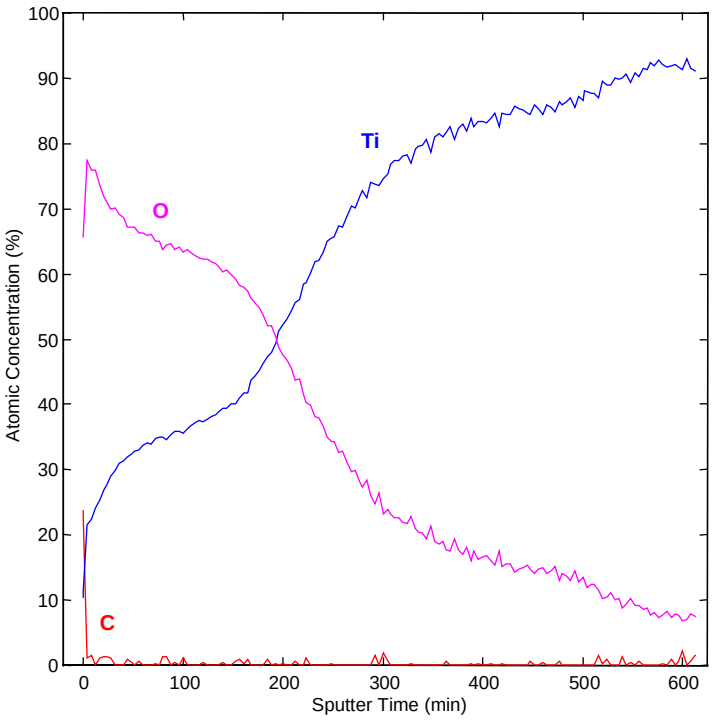

Fig. 12. Depth profile of the in-situ specimen after 5.3 years testing in the Asse salt mine at 190 °C. The experimental sputter rates amount to 0.12 nm/min for TiO_2 and 0.14 nm/min for Ti

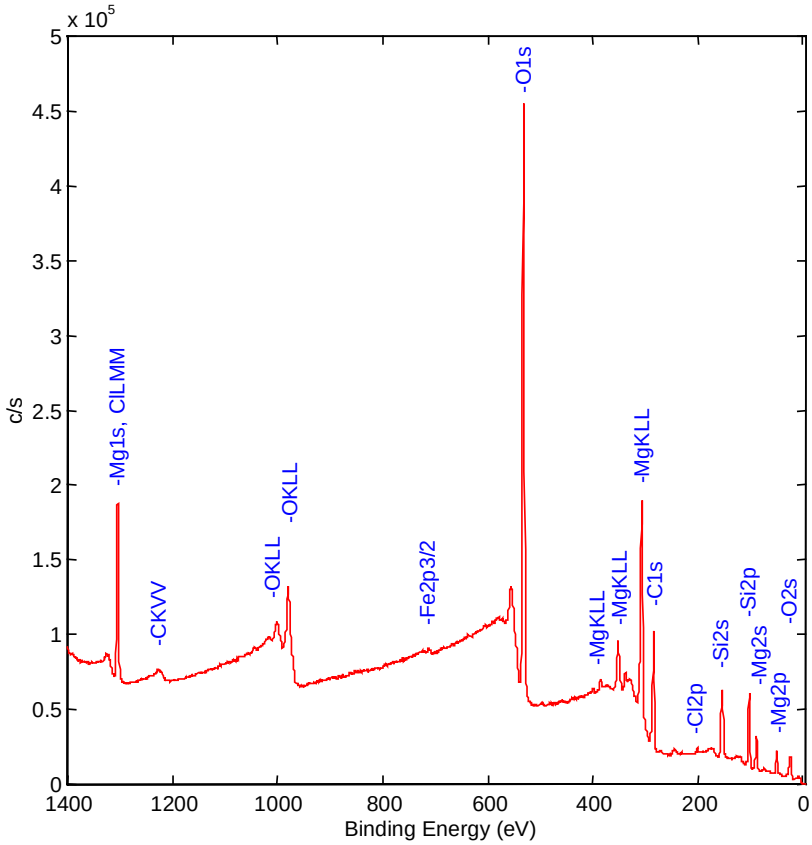

Fig. 13

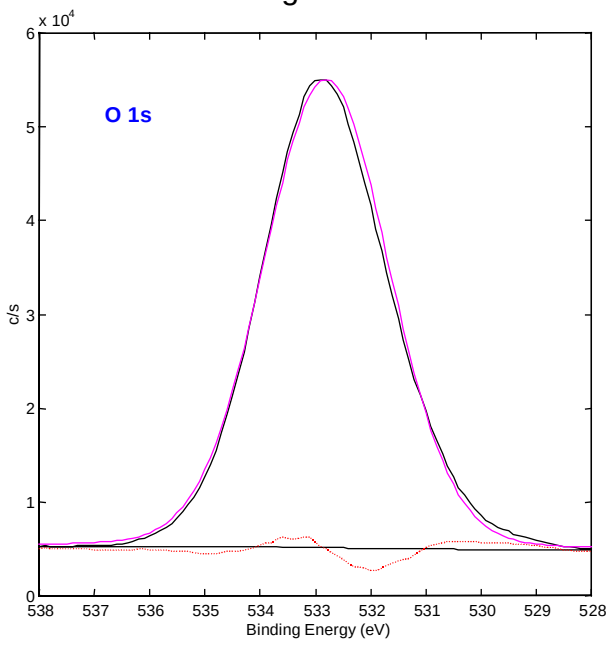

Fig. 14

Figs. 13 - 14. XPS survey spectrum (Fig. 13) and O1s spectrum (Fig. 14) of the free corroded surface of a Ti99.8-Pd specimen (244 days in Q-brine at 150 °C and 10 Gy/h). Titanium is not detected on the unsputtered surface

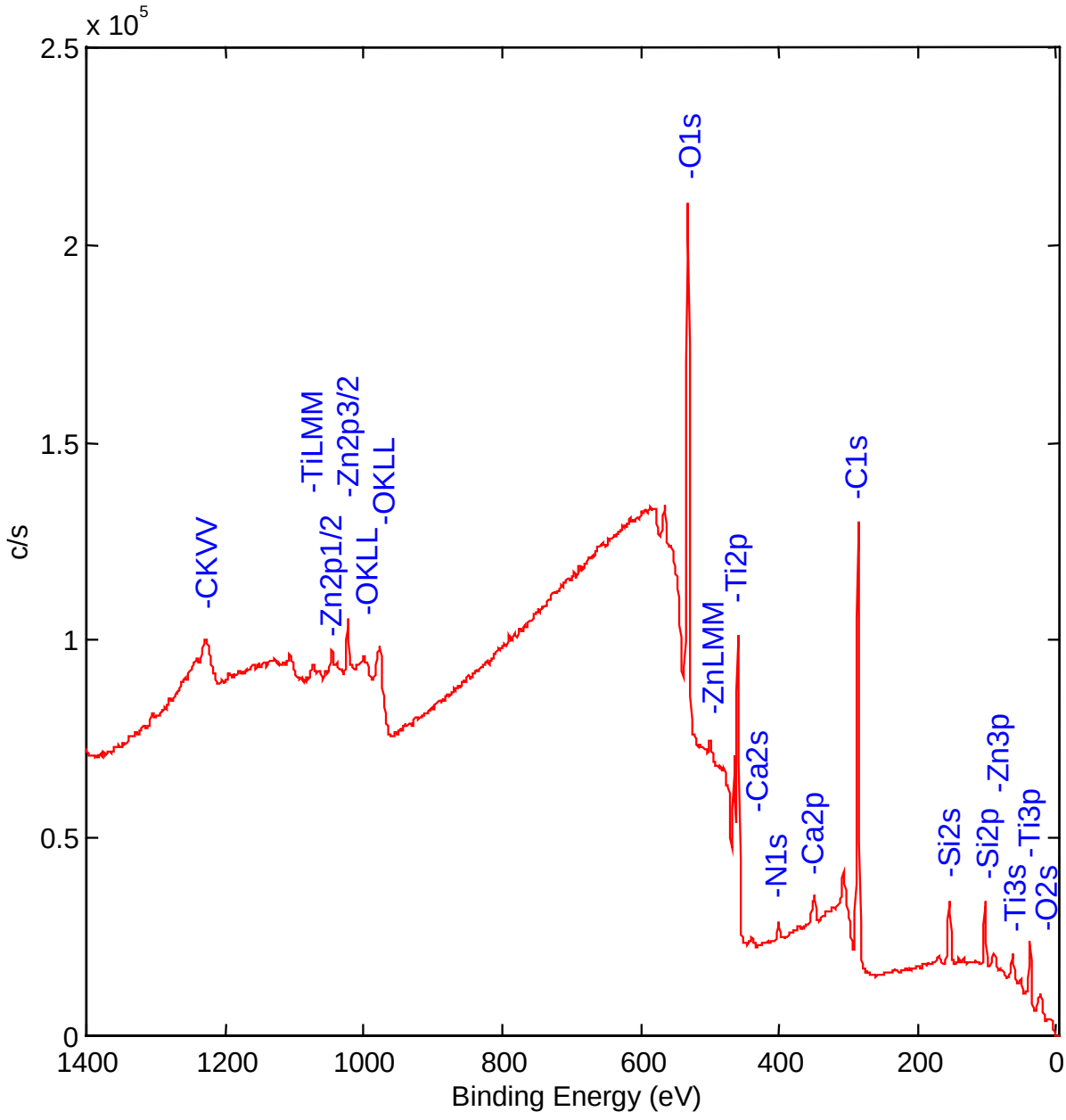

Fig. 15. XPS survey spectrum of the crevice surface of a Ti99.8-Pd specimen (244 days in Q-brine at 150 °C and 10 Gy/h)

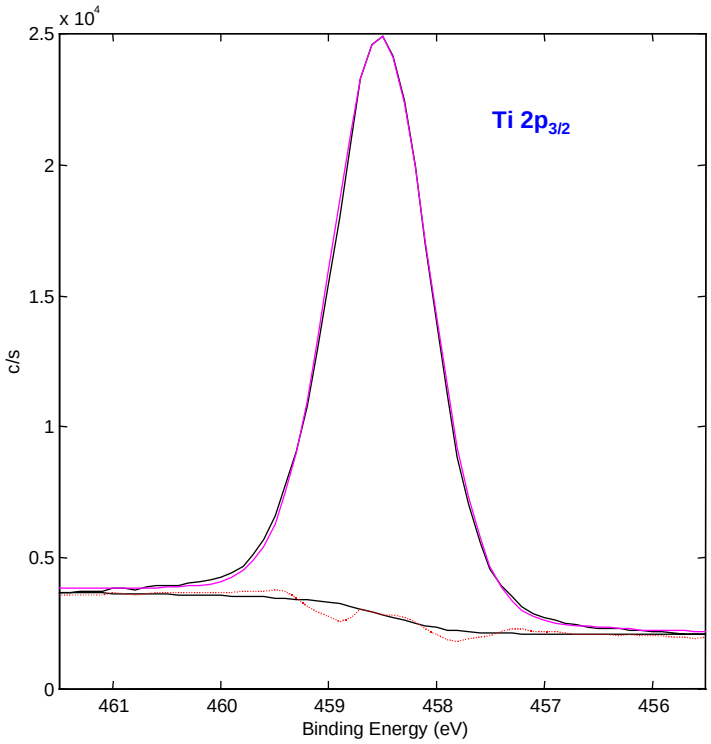

Fig. 16

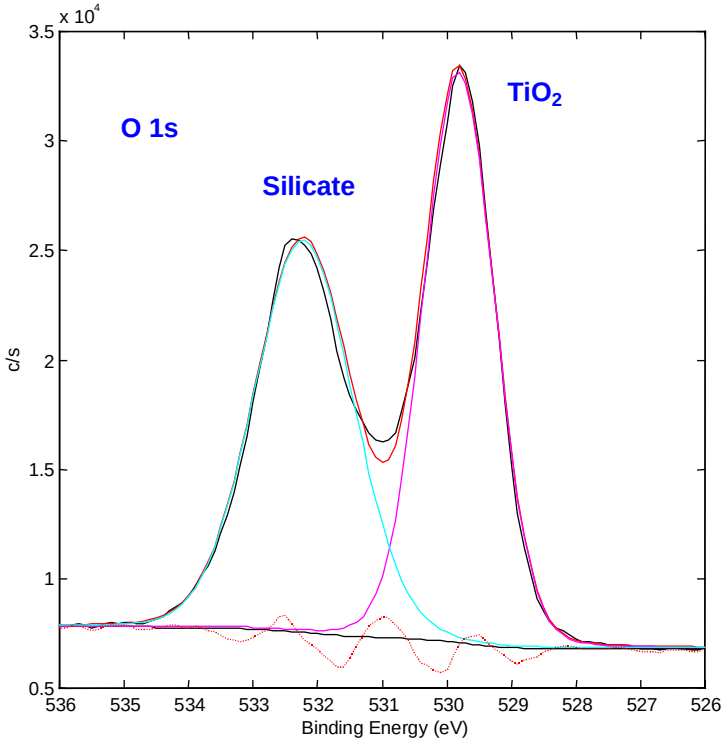

Fig. 17

Figs. 16 - 17. $Ti2p_{3/2}$ (Fig. 16) and O1s (Fig. 17) spectra of the crevice surface of a Ti99.8-Pd specimen (244 days in Q-brine at 150 °C and 10 Gy/h)

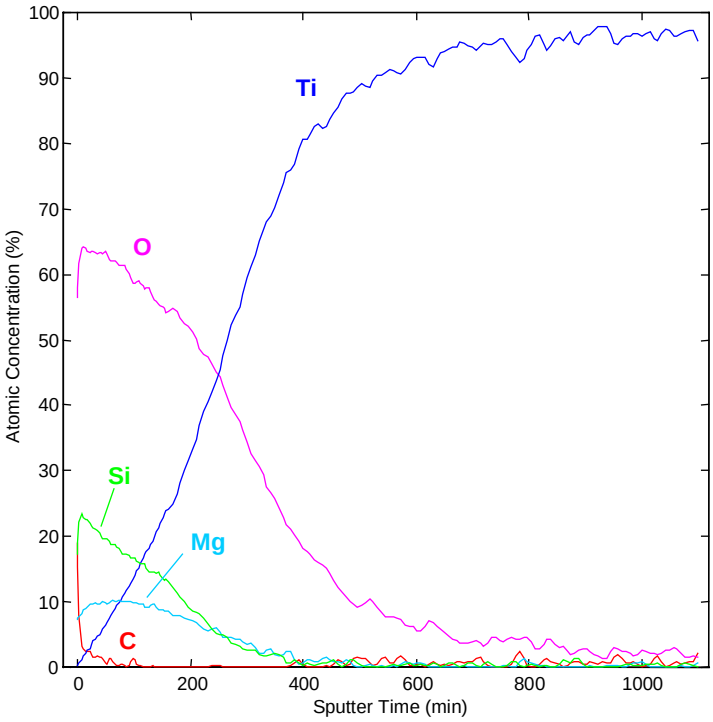

Fig. 18

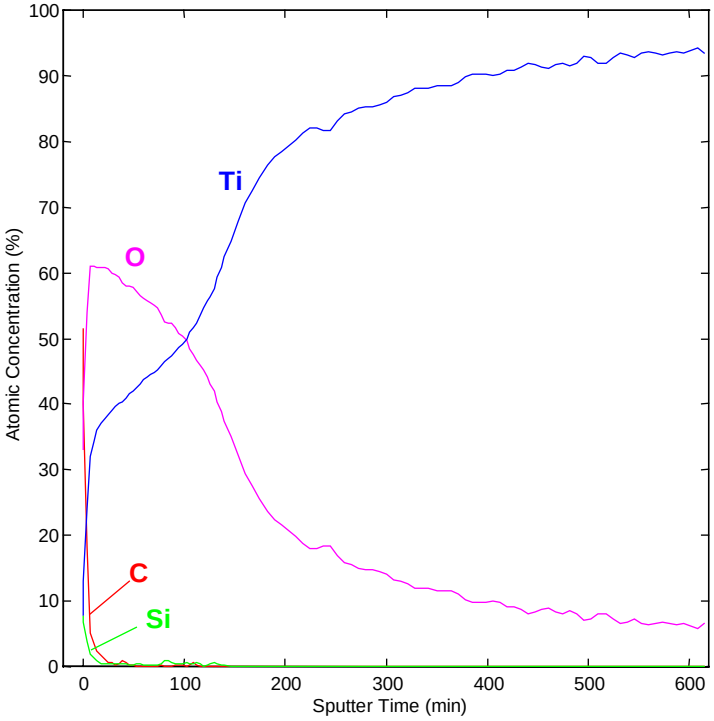

Fig. 19

Figs. 18 - 19. Depth profiles of the free corroded (Fig. 18) and crevice surface (Fig. 19) of a Ti99.8-Pd specimen (244 days in Q-brine at 150 °C and 10 Gy/h). The experimental sputter rates amount to 0.5 nm/min for TiO_2 and 0.58 nm/min for Ti